

# The Application of Quadrilateral Finite Elements for the Simulation of Recess T-gate MESFETs and HEMTs

Asen Asenov, Don Reid, John R. Barker, Nigel Cameron, and Steve P. Beaumont

Nanoelectronics Research Centre,  
Department of Electronics and Electrical Engineering  
University of Glasgow,  
Glasgow, G12 8QQ, UK

## Abstract

In this paper we present a new finite element approach for the simulation of recessed T-gate MESFETs and HEMTs based on quadrilateral finite elements. The discretization of the current continuity equation, which is the crucial part of the simulation, is followed in details. Two simulation examples - a 200 nm gate length MESFET and a  $\delta$ -doped pseudomorphic HEMT illustrates the usefulness of the adopted approach.

## I. Introduction

The performance of the modern nanometer-scale MESFETs and HEMTs becomes strongly affected by device parasitics such as coupling capacitances and access resistances [1]. In recessed gate devices these parasitics are critically affected by the shape and surface condition of the recess region. In addition the T-gate process designed to reduce the gate series resistance [2] may also reinforce the parasitic capacitances. Although Hydrodynamic [3] and Monte Carlo [4] simulation programs are making significant progress in properly describing the non-equilibrium transport phenomena in compound FETs, the real shape of the gate recess is generally poorly modelled, assuming planar or rectangular simulation domains. Surface effects are also either neglected or modelled by fixing the surface potential or by increasing the surface doping. Yet it is well known that this effects can in many cases have a more profound impact on device DC characteristics and high frequency performance than the transport details in the 'intrinsic' region under the gate.

In this paper we describe the implementation of a finite element approach based on quadrilateral finite elements for a precise description of the device's geometry and the realistic inclusion of the surface effects in the simulation of recessed gate MESFETs and HEMTs. Several simulation examples illustrate the work of the developed on this basis Heterojunction 2D Finite element (H2F) simulator.

## II. Model Description and Discretization

The heterojunction compound semiconductor device model equations used in the current version of H2F for steady state simulation include Poisson's equation and electron current continuity equation in a drift diffusion approximation

$$\nabla \cdot [\epsilon(\vec{r}) \nabla \psi] = -\rho(\vec{r}) \quad (1)$$

$$\nabla \cdot \vec{J}_n = 0 \quad (2)$$

$$\vec{J}_n = -e\mu_n \nabla \psi_1 + eD_n \nabla n \quad (3)$$

$$\psi_1 = \psi + \frac{\chi}{q} + \frac{kT}{q} \ln(N_c) \quad (4)$$

where all symbols have their usual meaning. While this approach is unable to describe precisely the device's transport, in many cases it is justified by the need to accurately predict the device parasitics.

A great deal of attention has been paid to the proper handling of the surface effects in the simulation. The charge term in the Poisson's equation is given by

$$\rho(\vec{r}) = q(N_{bulk}^i + \delta(\perp)N_{int}^i + p - n) \quad (5)$$

Where  $N_{bulk}^i$  and  $N_{int}^i$  represent charged bulk and interface states respectively. The symbol  $\delta(\perp)$  indicates that  $N_{int}^i$  is surface charge which may be placed along any (in the general case curvilinear) interface in the device. Similar to the bulk model the generalised interface trap model includes acceptor and donor like states with an arbitrary energy position whose occupation depends on the quasi-Fermi level and the potential variations. The simulation domain includes the space above the semiconductor surface providing a proper interaction between the charge on the surface states and the spreading surface potential.

Quadrilateral finite elements have been used for the discretization. The grid is generated by appropriate deformation of originally rectangular sub domains. Fig. 1 *a,b* illustrates this procedure for the gap between the gate and the cap layer of a recessed gate FET

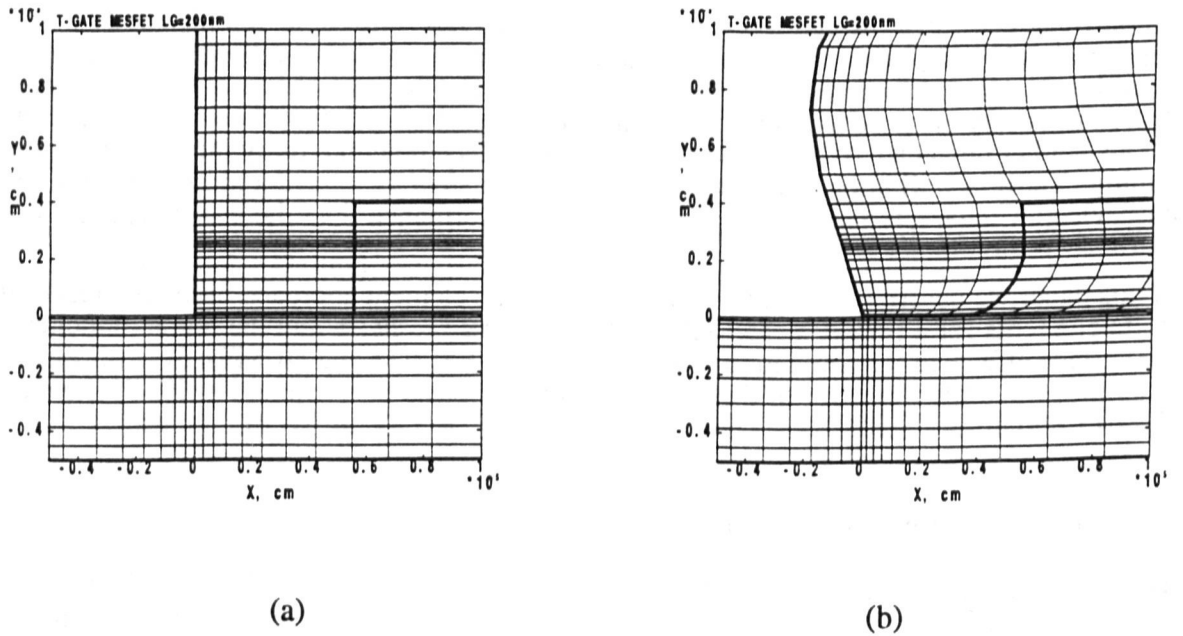


Fig. 1 Generation of the quadrilateral grid in the recess gate region. (a) the initial rectangular grid (b) the quadrilateral grid after suitable deformation

The Galerkin finite element method has been adapted to solve the Poisson's equation. The corresponding integration over the quadrilateral elements during the discretization was carried out by a linear isoparametric mapping (Fig. 3). A control volume method has been adopted [5] for the discretization of the current-continuity equation (Fig. 4). In this approach each quadrilateral element is divided into four subelements and the discretization is carried out balancing the current flowing in and out of the subelements attached to a given condensation point. Thus for vertex 1 (See Fig. 4)  $I_{41} - I_{21} = 0$ . A central point integration is used to calculate

the current through each of the subelement sides. For example  $I_{12}=d_1J_{12}$ , where the current density  $J_{12}$  is approximated by the standard Gummel expression.

$$J_{12} = \frac{D_{AB}}{l_1} \left[ \text{ber} \left( \frac{q\Delta\psi_{AB}}{kT} \right) n_A - \text{ber} \left( \frac{-q\Delta\psi_{AB}}{kT} \right) n_B \right] \quad (6)$$

The growth functions involved in the derivation of this expression are also used for interpolation of the electron concentration along the sides of the element. The electron concentration in point A for example is given by

$$n_A = w_{A1}n_1 + w_{A4}n_4 \quad (7)$$

where

$$w_{A4} = \frac{x_{4A} \text{ber} \left( \frac{q\Delta\psi_{14}}{kT} \right)}{\text{ber} \left( \frac{q\Delta\psi_{14}x_{4A}}{kTl_4} \right)} \quad (8)$$

and

$$w_{A1} = 1 - w_{A4} \quad (9)$$

It has been found that this discretization is stable for arbitrary shapes of the quadrilateral elements and does not leads to the spikes typical for obtuse triangles. The same approach may be used for discretization of the momentum and energy conservation equation in the quasi-hydrodynamic transport treatment.

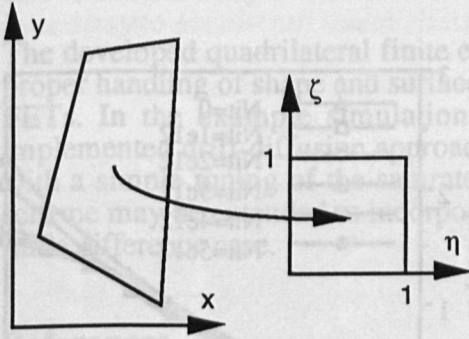


Fig. 2 Linear isoparametric mapping

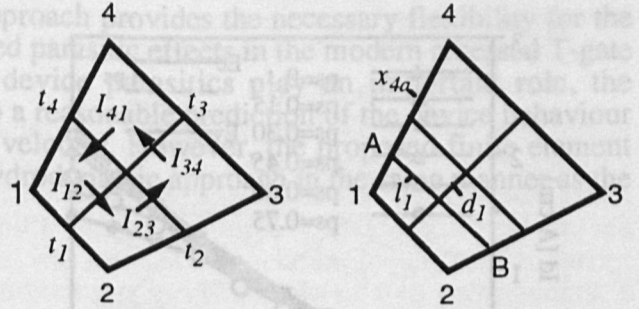


Fig. 3 Discretization of the current continuity equation

The grid generation preserves the number of grid points in lateral and vertical directions and leads to a regular nine diagonal matrix of the discretized equations. A Fast Incomplete LU Factorisation Biconjugate Gradients (ILUBCG) solver is used for the numerically intensive iterations. The solution of the Poisson's equation involves only a few biconjugate gradient steps per Newton iteration that significantly reduces the total computation time. The convergence problems related to the strongly localised, potential dependent interface charge have been resolved by appropriate dumping. ILUBCG also solves without complication the discretized current continuity equation.

Although H2F is 'serial' code, by using a pipeline filesaver, multiple copies of the program can be run concurrently on MIMD machines (in our case a Parsytec Model 64 transputer system), calculating in parallel, separate sets of input device parameters. This extends dramatically the capability of the simulator for real design work such as structure optimisation, sensitivity analysis and yield prediction where several hundred simulations are often carried out during single investigation.

### III. Examples

Two simulation examples illustrate the application of the developed quadrilateral finite element approach for the simulation of complex shaped devices. The first example is concerned with the simulation of a 200 nm gate-length state of the art MESFET, fabricated in the Nanoelectronics Research Centre at the University of Glasgow [6]. The flexibility of the quadrilateral grid is illustrated in Fig. 4 where the cross sectional photograph of the device is compared with the corresponding H2F simulation domain.

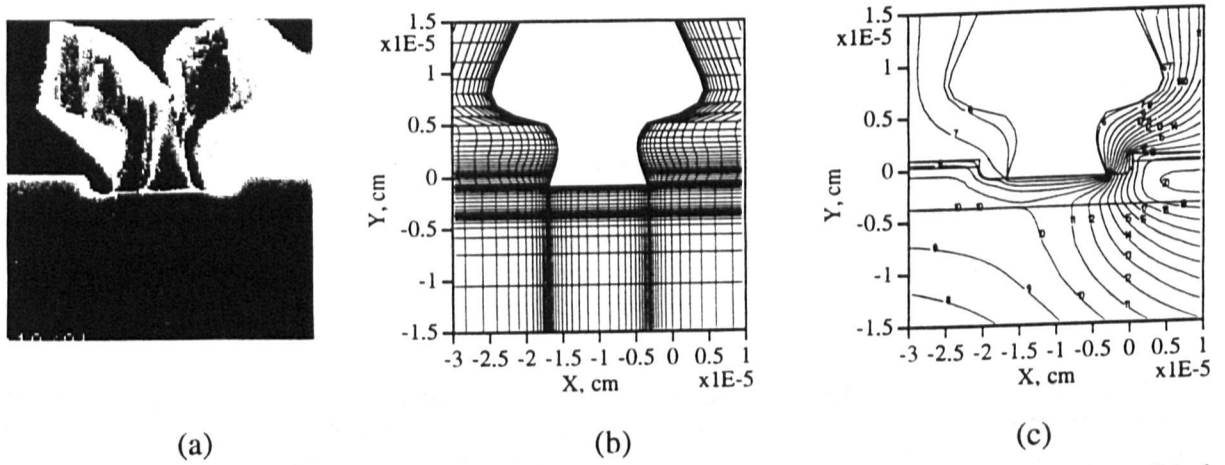


Fig. 4 Simulation of a 200 nm gate length MESFET. (a) Cross sectional SEM view (b) the corresponding finite element grid (c) potential distribution at  $V_G = -0.4V$  and  $V_D = 2.5 V$

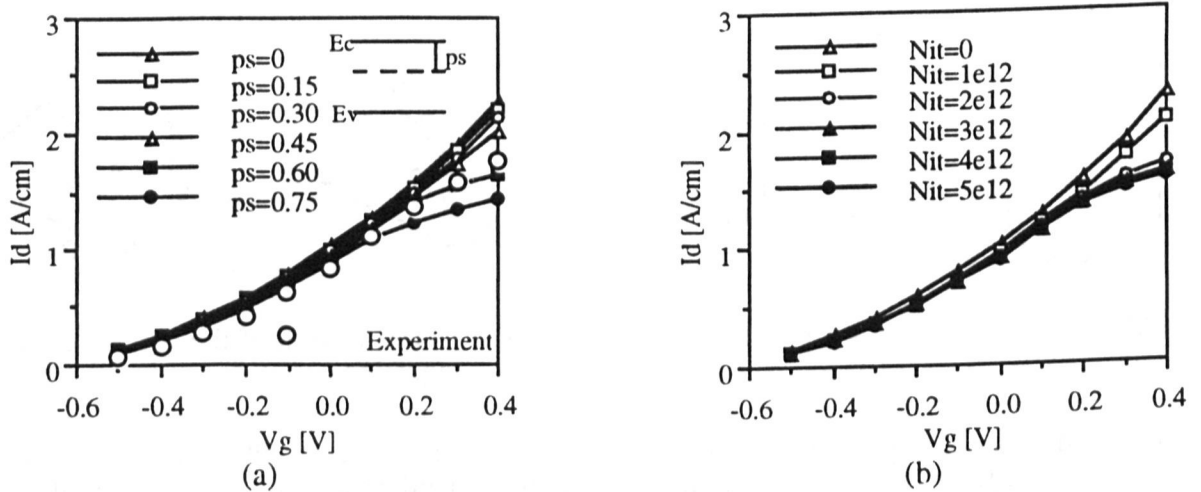


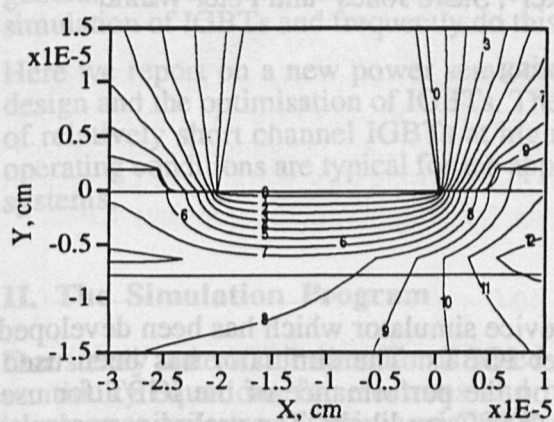
Fig. 5 Simulated and measured  $I_D$ - $V_D$  characteristics of the device illustrated in Fig. 4. (a) influence of acceptor type surface states position  $P_s$  (b) influence of the surface state density  $N_{it}$

The influence of the position and the density of these surface states on the device's  $I_D$ - $V_G$  characteristics for the MESFET shown in Fig. 4 is given in Fig 5 *a,b*. Our experimental measurements are in good agreement with the expected position and states density  $P_s = 0.6 eV$  and  $N_{it} = 2e12 cm^{-2}$ .

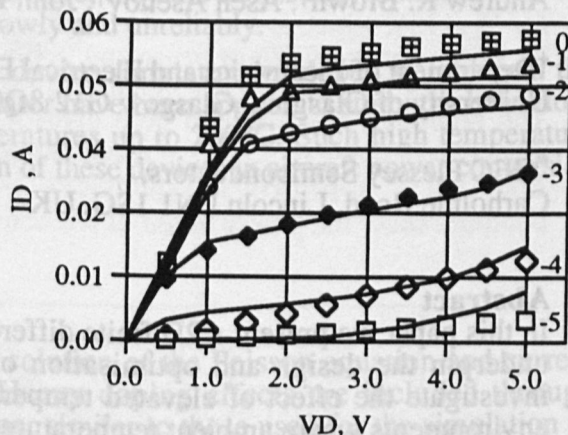
The second example is the simulation of a delta-doped pseudomorphic HEMT whose behaviour is significantly influenced by the series resistances introduced by an undoped cap layer (Fig. 6). Although the drift diffusion approach underestimates the current, it has been found that by



adjusting the saturation velocity in the mobility model (to  $1.4 \times 10^7$  cm/s in this case) the measured characteristics can be acceptably matched.



(a)



(b)

Fig. 6 Simulation of 200 nm gate length pseudomorphic HEMT (a) device structure and potential distribution at  $V_G=3.5$  V and  $V_D=2.5$  V (0 correspond to -4 V and the increment is 0.5 V) (b) measured (lines) and calculated (symbols)  $I_D - V_G$  characteristics

#### IV. Conclusions

The developed quadrilateral finite element approach provides the necessary flexibility for the proper handling of shape and surface associated parasitic effects in the modern recessed T-gate FETs. In the example simulations, where device parasitics play an important role, the implemented drift-diffusion approach leads to a reasonable prediction of the device behaviour with a simple tuning of the saturated carrier velocity. However, the proposed finite element scheme may be extended to incorporate the hydrodynamic approach in the same manner as the finite difference case.

#### References

- [1] P.H. Ladbrooke, A.J. Hill and J.P. Bridge, "Fast FET and HEMT Solvers for Microwave CAD", J. Microwave and Millimetre-Wave Computer Aided Eng., Vol. 3, No. 1, pp.37-60, 1993.
- [2] P.C. Chao, P.M. Smit, S.C. Plamaeteer, and J.C.M. Hwang, "Electron Beam Fabrication of GaAs Low-Noise MESFET's Using a New TriLauer Resist Technique", IEEE Trans. Electron Dev., Vol. ED-32, No. 6, pp.1042-1045, 1985.
- [3] J.-R. Zhou and D.K. Ferry, "Simulation of Ultra-Small GaAs MESFET Using Quantum Moment Equations", IEEE Trans. Electron Dev., Vol 39, No. 3, pp.473-478, 1992.
- [4] I.C. Kizilyalli, M. Artaki and A. Chandra, "Monte Carlo Study of GaAs/ $\text{Al}_x\text{Ga}_{1-x}\text{As}$  MODFET's: The Effect of  $\text{Al}_x\text{Ga}_{1-x}\text{As}$  composition", IEEE Trans. Electron Dev., Vol. 38, No. 2, pp.197-206, 1991.
- [5] A. Asenov and E. Stefanov, "IMPEDANCE 2.0: A Flexible Concept for Process and Device Simulation", Proc. ISPPM, pp.272-286, Varna 1989.
- [6] N.I. Cameron, G. Hopkins, I.G. Thayne, S.P. Beaumont, C.D.W. Wilkinson, M. Holland, A.H. Keanand and C.R. Stanley, "Selective Reactive Ion Etching of GaAs/AlGaAs Metal-Semiconductor Field Effect Transistors", J. Vac Sci. Technol. B, Vol. 9 p.3538, 1991.